Fluid Models and Parameter Sensitivities: Computations, and Applications

L. Davis¹, M. Neda², Fran Pahlevani³, and J. Waters⁴

¹Department of Mathematics, Montana State University, Bozeman, MT 59717
 ²Department of Mathematics, University of Nevada, Las Vegas, NV 89154
 ³Division of Science and Engineering, Penn State Abington, Abington, PA 19001
 ⁴Department of Mathematics, University of Nevada, Las Vegas, NV 89154

Presenting author: Fran Pahlevani Corresponding author: fxp10@psu.edu

Abstract

Fluid models were developed as an alternative to the Navier-Stokes equations to avoid computational complexity especially in case of turbulent flows. Model errors due to the sensitivity of a model to user-elected parameters become an immediate concern. Quantifying this error and assessing the reliability of the model given a parameter value are essential to understanding and using model predictions within an engineering design process. This paper presents an overview of sensitivity computations of three fluid models namely Eddy Viscosity Model, Leray-Alpha Model, and Time Relaxation Model to the variations of different model parameters. The 2D Cavity problem is used to numerically illustrate the application of sensitivity computations in identifying the range of parameter values for which the fluid model can be considered a reliable approximation. In addition, testing on the 2D flow around a cylinder, our numerical results supports the idea that sensitivity information can incorporate the effects of unresolved scales on flow functionals that leads to an improved estimation.

1 Introduction

Numerous types of fluid flows are formulated by Navier-Stokes Equations (NSE) based on the fluid velocity and pressure. When we solve these equations numerically, the flow velocity consists of different scales and eddies. Numerical simulations of NSE are used for two major purposes. One is to understand the physical mechanism of the fluid and the other is to predict the flow characteristics in applications. Both cases require a numerical simulation producing data of very high accuracy. Since the precision of generated data depends on the level of selected resolution, for the best possible numerical result the simulation has to take into account all the space-time scales in the fluid dynamics. As known by Kolmogorov's law, the required number of mesh points in space per time step in a three dimensional flow is related to the Reynolds number, Re, and it is $O(Re^{9/4})$. This leads to the fact that fluid flows

with large enough Re are expensive simulations regarding both the required storage and the running time. Technically Direct Numerical Simulation (DNS) is computationally infeasible especially in the case of turbulent flows when the range of velocity scales is very large. As an alternative, regularization models of NSE were developed to allow for computational efficiency in case of high Re numbers. These models are mostly based on a technique that uses a filtering procedure on NSE, ultimately solving the equations for only large scale velocities. Removing some scales from the fluid system not only affects the accuracy of the numerical data but also their reliability that leads to the major issue of model errors and uncertainty in model predictions. This raises concerns particularly in applications where important decisions are made; see [31, 19, 29, 3]. The model reliability becomes an issue especially when the fluid model is sensitive with respect to the variation of a user-elected parameter. Such parameters appear to be inevitable in the process of modeling. Filter length scale is a simple example to be named. To this end, parameter sensitivity analysis is considered a technique to asses the reliability of the computed flow solution using a fluid model. Sensitivity analysis of a flow system is defined as the computation of derivative of flow variables with respect to model parameters upon which the response of the flow system explicitly and/or implicitly depends [5, 16]. A natural approach to obtain flow sensitivity known as Continuous Sensitivity Equation Method (CSEM) is to form a continuous equation for the designated sensitivity and then numerically solving it. CSEM has been used in sensitivity calculations of flows with respect to various flow-related parameters; see for example [4, 6, 14].

This paper provides a summery first on the use of CSEM in computing sensitivity of three specific fluid models, namely a subgrid Eddy Viscosity Model (EVM), Leray-Alpha Model (LAM), and Time Relaxation Model (TRM) with respect to a model parameter, second the use of sensitivity information in quantifying the model reliability, and last on the application of the sensitivity computation in improving flow functionals. An extensive study of these topics are presented by authors in [28, 26, 27].

2 Continuous Sensitivity Equation

In this section we introduce the equations for EVM, LAM, and TRM, and derive the sensitivity equations with respect to variations of a model parameter for each. In the first two models, the parameter of consideration is the filter length scale and in the latter, it is the time relaxation coefficient whose value specifies how strongly the growth of fluctuations are truncated.

The discussed subgrid EVM in this paper was first introduced by Layton [21]. The analysis and numerical computations of two first-order semi-implicit schemes for EVM and NSE are persented in [10]. An error analysis of this model using discontinuous polynomial approximations can be found in [20]. An explicit sensitivity study of this model with application to quantifying model reliability is given in [28].

In 1934, for the first time Leray introduced a regularization of NSE on the nonlinear term using a Gaussian filter and proved the existence and uniqueness of strong solutions to his model [24, 25]. In a reexamination of Leray model, the Gaussian filter was replaced by a differential filter and the theory and computations of this new model, LAM, were studied by different group of scientists [8, 9, 18, 33, 23, 7]. A computational study on the sensitivity of LAM with respect to the filter width is presented in [26].

TRM was originally developed from regularized Chapman-Enskog expansion of conserva-

tion laws by Rosenau [30], Schoehet and Tadmor [32]. The given TRM in this paper uses the van Cittert deconvolution in regularization term proposed by Stolz, Adams and Kleiser[1] who also extensively tested the model on compressible flows with shocks and turbulent flows [1, 2, 13]. An analysis of a discrete numerical scheme using a continuous finite element method can be found in [13].

EVM and TRM regularize the NSE by adding a stabilization term however LAM applies a regularization to the non-linear term in NSE. EVM is obtained by applying a filtering operator to the NSE that is an L^2 -orthogonal projection while the other two fluid models use a differential filter.

In the following equations for EVM, LAM, and TRM, \mathbf{u} and p represent velocity and pressure respectively, \mathbf{f} is the body force, and $\nu > 0$ is the kinematic viscosity, which is inversely proportional to Re. In the corresponding sensitivity equations for all models, \mathbf{s} and r represent the velocity and pressure sensitivities with respect to the designated parameter, and $\overline{\mathbf{u}}$ stands for the average velocity. In all the equations, Ω is considered to be a bounded, simply connected two- or three-dimensional domain with polygonal boundary $\partial\Omega$.

Definition 2.1. Let \mathbf{u} , $\overline{\mathbf{u}}$, and p be the flow variables as velocity, average velocity, and pressure, respectively. The sensitivity of these variables to variations of a designated model parameter η is defined to be the flow variable derivative with respect to η .

$$\mathbf{s} = \frac{\partial \mathbf{u}}{\partial \eta}, \mathbf{w} = \frac{\partial \overline{\mathbf{u}}}{\partial \eta}, \text{ and } r = \frac{\partial p}{\partial \eta}$$

Note that all the models are for incompressible flows with zero boundary condition given as,

$$\begin{array}{rcl} \nabla \cdot \mathbf{u} & = & 0, & \text{in } \Omega \times [0, T] \\ \mathbf{u} & = & 0, & \text{on } \partial \Omega \times [0, T] \\ \mathbf{u}(x, 0) & = & \mathbf{u}_0(x), & \text{in } \Omega. \end{array}$$

Assuming that the velocity initial condition is dependent free from the designated model parameter, the sensitivity of the above equations appears as the following,

$$\nabla \cdot \mathbf{s} = 0, \text{ in } \Omega \times [0, T]$$

$$\mathbf{s} = 0, \text{ on } \partial \Omega \times [0, T]$$

$$\mathbf{s}(x, 0) = 0, \text{ in } \Omega.$$

In the following, we introduce the equations for EVM, LAM, and TRM.

2.1 Eddy Viscosity Model

The EVM over the time interval [0, T] is outlined as following

$$\mathbf{u}_t + \mathbf{u} \cdot \nabla \mathbf{u} - \nu \Delta \mathbf{u} + \nabla p - \alpha \nabla \cdot (\nabla \mathbf{u} - \overline{\mathbf{u}}) = \mathbf{f}, \text{ in } \Omega \times (0, T].$$
 (2.1)

Here for any $\mathbf{v} \in (L^2(\Omega))^d$, d = 2 or 3, $\overline{\mathbf{v}} = P(\nabla \mathbf{v})$, where $P : L^2(\Omega) \to L$ is an L^2 -orthogonal projection, defined on a chosen subspace of $L^2(\Omega)$ [21], denoted by L. The parameter α known as the eddy viscosity coefficient, corresponds to the filter length scale. Therefore its values vary between 0 and 1 with $\alpha = 0$ corresponding to the Navier-Stokes equations.

For simplicity, it is assumed that the L^2 -orthogonal projection P is differentiable with respect to parameter α . Since this operator is a linear operator, using the chain rule it can be easily shown that the operator P commutes with differentiation with respect to α . Implicitly differentiating (2.1) with respect to α produces the following sensitivity equation.

$$\mathbf{s}_t + \mathbf{u} \cdot \nabla \mathbf{s} + \mathbf{s} \cdot \nabla \mathbf{u} - \nu \Delta \mathbf{s} + \nabla r - \alpha \nabla \cdot (\nabla \mathbf{s} - \overline{\mathbf{s}}) = \nabla \cdot (\nabla \mathbf{u} - \overline{\mathbf{u}}), \text{ in } \Omega \times (0, T]. \tag{2.2}$$

2.2 Leray-Alpha Model

The regularization of the NSE by LAM is formulated as following

$$\mathbf{u}_t + \overline{\mathbf{u}} \cdot \nabla \mathbf{u} - \nu \triangle \mathbf{u} + \nabla p = \mathbf{f}, \text{ in } \Omega \times (0, T]$$
 (2.3)

where $\overline{\mathbf{u}}$ is obtained from the differential filter,

$$-\alpha^2 \triangle \overline{\mathbf{u}} + \overline{\mathbf{u}} = \mathbf{u}, \text{ in } \Omega$$
$$\overline{\mathbf{u}} = 0, \text{ on } \partial \Omega. \tag{2.4}$$

Sensitivity equations of LAM with respect to variations of parameter α are given as

$$\mathbf{s}_t + \mathbf{w} \cdot \nabla \mathbf{u} + \overline{\mathbf{u}} \cdot \nabla \mathbf{s} + \nabla q - \nu \triangle \mathbf{s} = \mathbf{f}, \text{ in } \Omega \times (0, T]$$
 (2.5)

In (2.5), w is obtained from the sensitivity equation of the differential filter in (2.4).

$$-\alpha^{2} \triangle \mathbf{w} + \mathbf{w} = -\frac{2}{\alpha} (\mathbf{u} - \overline{\mathbf{u}}) + \mathbf{s}, \text{ in } \Omega$$

$$\mathbf{w} = 0, \text{ on } \partial \Omega$$
 (2.6)

2.3 Time Relaxation Model

Similar to EVM, TRM consists of the Navier-Stokes equations with an addition of a stabilization term to the momentum equation and is defined by

$$\mathbf{u}_t + \mathbf{u} \cdot \nabla \mathbf{u} + \nabla p - \nu \Delta \mathbf{u} + \chi (\mathbf{u} - G_N \overline{\mathbf{u}}) = \mathbf{f}, \text{ in } \Omega \times (0, T]$$
 (2.7)

Here, $\overline{\mathbf{u}}$ stands for an averaged function of \mathbf{u} by filter width α satisfying the differential filter given in (2.4). The operator G_N is the continuous van Cittert deconvolution operator, where N denotes the deconvolution order, and for any $\mathbf{v} \in H_0^1(\Omega)$ is defined as following [22],

$$G_N \mathbf{v} := \sum_{n=0}^N (I - G)^n \mathbf{v}.$$

For the zero and first order of deconvolution, we have the van Cittert deconvolution as $G_0 \mathbf{v} = \mathbf{v}$, and $G_1 \mathbf{v} = 2\mathbf{v} - \overline{\mathbf{v}}$, respectively. As discussed in [12], higher order of deconvolution produces

more accurate approximations but it becomes costly in terms of computational time. All the studies in this paper are carried out for the fundamental case when the order of deconvolution is zero, i.e. N=0. The action of the term $\chi(\mathbf{u}-G_N\overline{\mathbf{u}})$ is to drive fluctuations lower than $O(\alpha)$ to zero as $t\to\infty$.

Differentiating TRM implicitly with respect to parameter χ gives the following equations for sensitivity,

$$\mathbf{s}_t + \mathbf{u} \cdot \nabla \mathbf{s} + \mathbf{s} \cdot \nabla \mathbf{u} + \nabla r - \nu \Delta \mathbf{s} + (\mathbf{u} - \overline{\mathbf{u}}) + \chi(\mathbf{s} - \mathbf{w}) = 0, \text{ in } \Omega \times [0, T]$$
 (2.8)

where **w** is the solution of the following sensitivity equation obtained by differentiating (2.4) with respect to parameter χ ,

$$-\alpha^2 \triangle \mathbf{w} + \mathbf{w} = \mathbf{s}, \text{ in } \Omega,$$

$$\mathbf{w} = 0, \text{ on } \partial \Omega.$$
 (2.9)

3 The Algorithms and Discretizations

This section is devoted to introducing the basis for deriving a finite element approximation of \mathbf{u} in (2.1), (2.3)-(2.6), and (2.7) as well as \mathbf{s} in (2.2), (2.5)-(2.6), and (2.8)-(2.9).

As it can be seen in (2.2), (2.5)-(2.6), and (2.8)-(2.9), velocity \mathbf{u} , and its average $\overline{\mathbf{u}}$ appear in the sensitivity equations. Therefore in computing sensitivities one needs to couple the sensitivity equations with the corresponding model. Given \mathbf{u} , and $\overline{\mathbf{u}}$ the sensitivity equations are linear equations. Therefore sensitivity can be calculated in a very inexpensive manner once the numerical method for computing \mathbf{u} in each model is constructed. The bulk of the work for the computation is in the implementation of equations (2.1), (2.3), and (2.7). Once that is accomplished, the incorporation of the sensitivity equations in (2.2), (2.5), and (2.8) into a numerical algorithm that computes both \mathbf{u} and \mathbf{s} is straightforward. As one can easily observe, all the sensitivity data structures are virtually the same or very similar to one computed from the fluid model.

Following is the notation for function spaces used in finite element theory,

$$\mathbf{X}^h \subset X = H_0^1(\Omega) := \{ \mathbf{v} \in H^1(\Omega) : \mathbf{v}|_{\partial\Omega} = 0 \},$$

$$Q^h \subset Q = L_0^2(\Omega) := \{ q \in L^2(\Omega) : \int_{\Omega} q = 0 \}.$$

For the treatment of convective and diffusive terms in the variational formulation of equations, we use the following bilinear and trilinear forms.

$$a(\mathbf{u}, \mathbf{v}) = (\nabla \mathbf{u}, \nabla \mathbf{v})$$

$$b(\mathbf{u}, \mathbf{v}, \mathbf{w}) = (\mathbf{u} \cdot \nabla \mathbf{v}, \mathbf{w})$$

$$b^*(\mathbf{u}, \mathbf{v}, \mathbf{w}) = \frac{1}{2}(\mathbf{u} \cdot \nabla \mathbf{v}, \mathbf{w}) - \frac{1}{2}(\mathbf{u} \cdot \nabla \mathbf{w}, \mathbf{v}).$$

Next we apply the following classical steps to EVM, LAM, TRM, and their sensitivity equations.

- Variational Formulation: The equations (2.1)- (2.2), (2.3)-(2.6), and (2.7)-(2.9) are reformulated in a weak form after multiplication by a suitable set of test functions, $\mathbf{v} \in X$ and $\lambda \in Q$, and performing an integration upon the domain. At this stage, the integration by parts is used to reduce the order of differentiation for solutions, \mathbf{u} and \mathbf{s} .
- Discretization in Space: Let $h \in (0,1]$, tending to zero, be the spatial mesh size, then $V^h = \{ \mathbf{v} \in X^h : (\lambda, \nabla \cdot \mathbf{v}) = 0, \text{ for all } \lambda \in Q^h \}$ is a finite dimensional subspace of X^h . Since (V^h, Q^h) fulfills the inf-sup or Babuska-Brezzi stability condition, by selecting the test functions from these spaces the pressure p_h can be eliminated from the system in its discrete form; see [15]. In the resulting equations, for each $t \in [0, T]$, \mathbf{u}_h and \mathbf{s}_h are solved in V^h .
- Discretization in Time: We start with partitioning the time interval [0,T] into N subintervals $[t^n, t^{n+1}]$ of length $\Delta t = \frac{T}{N}$. Then at each time level t^n , an approximation to \mathbf{u} and \mathbf{s} , denoted by \mathbf{u}_h^n and \mathbf{s}_h^n respectively, are obtained.

3.1 Eddy Viscosity Model

Here we specifically explain how the stabilization term in EVM and its sensitivity are estimated in our calculations. By definition $\overline{\mathbf{v}}$ is an L^2 -orthogonal projection of $\nabla \mathbf{v}$ onto L, therefore it can be obtained by the following equation

$$(\nabla \mathbf{v} - \overline{\mathbf{v}}, l) = 0, \ \forall \mathbf{v} \in (L^2(\Omega))^d, l \in L.$$
(3.1)

In the spatial discretization form of (3.1), a multiscale spatial discretization is applied. Let h and H denote two different mesh widths (h < H). Then the space $L^H \subset L^2(\Omega)^{d \times d}$, d = 2 or 3, is considered as the space of large scales of the velocity that are numerically solved by EVM since H represents the coarse mesh size.

In the fully discrete form of EVM, a semi-implicit numerical scheme is applied. The convective term is computed using a backward-forward time-stepping method. Thus the equation reads as: Given \mathbf{u}_h^n , we seek \mathbf{u}_h^{n+1} satisfying

$$(\nabla \mathbf{u}_h^n - \overline{\mathbf{u}}_H^n, l) = 0,$$

$$\frac{1}{\Delta t}(\mathbf{u}_h^{n+1} - \mathbf{u}_h^n, \mathbf{v}) + (\nu + \alpha)a(\mathbf{u}_h^{n+1}, \mathbf{v}) + b(\mathbf{u}_h^n, \mathbf{u}_h^{n+1}, \mathbf{v}) - \alpha(\overline{\mathbf{u}}_H^n, \nabla \mathbf{v}) = (f^{n+1}, \mathbf{v}). \tag{3.2}$$

Similarly, given s_h^n , we find s_h^{n+1} such that

$$(\nabla \mathbf{s}_{h}^{n} - \overline{\mathbf{s}}_{H}^{n}, l) = 0,$$

$$\frac{1}{\Delta t} (\mathbf{s}_{h}^{n+1} - \mathbf{s}_{h}^{n}, \mathbf{v}) + (\nu + \alpha) a(\mathbf{s}_{h}^{n+1}, \mathbf{v}) + b(\mathbf{s}_{h}^{n+1}, \mathbf{u}_{h}^{n+1}, \mathbf{v}) + b(\mathbf{u}_{h}^{n+1}, \mathbf{s}_{h}^{n+1}, \mathbf{v})$$

$$-\alpha (\overline{\mathbf{s}}_{H}^{n}, \nabla \mathbf{v}) = (\overline{\mathbf{u}}_{H}^{n} - \nabla \mathbf{u}_{h}^{n}, \nabla \mathbf{v}). \tag{3.3}$$

An extensive numerical analysis of EVM in (3.2) and its sensitivity equation in (3.3) with further numerical tests can be found in [10, 28].

3.2 Leray-Alpha Model

In the discretization of the time derivative of LAM, the Crank-Nicolson method is used. For clarity in notation, we let $\mathbf{v}(t^{n+1/2}) = \mathbf{v}((t^{n+1}+t^n)/2)$ for the continuous variable and $\mathbf{v}^{n+1/2} = (\mathbf{v}^{n+1} + \mathbf{v}^n)/2$ for both, continuous and discrete variables.

Discrete approximation solutions of LAM, given by (2.3)-(2.4), on the time interval (0, T], is to find \mathbf{u}_h^{n+1} and $\overline{\mathbf{u}}_h^n$ such that

$$\alpha^{2}(\overline{\mathbf{u}}_{h}^{n}, \nabla \mathbf{v}) + (\overline{\mathbf{u}}_{h}^{n}, \mathbf{v}) - (\mathbf{u}_{h}^{n}, \mathbf{v}) = 0,$$

$$\frac{1}{\wedge t}(\mathbf{u}_{h}^{n+1} - \mathbf{u}_{h}^{n}, \mathbf{v}) + \nu a(\mathbf{u}_{h}^{n+1/2}, \mathbf{v}) + b^{*}(\overline{\mathbf{u}}_{h}^{n+1/2}, \mathbf{u}_{h}^{n+1/2}, \mathbf{v}) = (\mathbf{f}_{h}^{n+1/2}, \mathbf{v}). \tag{3.4}$$

Discrete approximation to the sensitivity equations (2.5) and (2.6) on the time interval (0, T], is to find \mathbf{s}_h^{n+1} and \mathbf{w}_h^n such that

$$\alpha^{2}(\nabla \mathbf{w}_{h}^{n}, \nabla v) + (\mathbf{w}_{h}^{n}, v) - (\mathbf{s}_{h}^{n}, \mathbf{v}) + \frac{2}{\alpha}(\mathbf{u}_{h}^{n} - \overline{\mathbf{u}}_{h}^{n}, \mathbf{v}) = 0,$$

$$\frac{1}{\wedge t}(\mathbf{s}_{h}^{n+1} - \mathbf{s}_{h}^{n}, \mathbf{v}) + \nu a(\mathbf{s}_{h}^{n+1/2}, \mathbf{v}) + b^{*}(\mathbf{w}_{h}^{n+1/2}, \mathbf{u}_{h}^{n+1/2}, \mathbf{v}) + b^{*}(\overline{\mathbf{u}}_{h}^{n+1/2}, \mathbf{s}_{h}^{n+1/2}, \mathbf{v}) = 0.$$
 (3.5)

3.3 Time Relaxation Model

Similar to LAM, the Crank-Nicolson numerical scheme is applied to TRM and its sensitivity equations. Therefore we obtain the following discretized finite element variational formulations. Find \mathbf{u}_h^{n+1} and $\overline{\mathbf{u}}_h^n$ satisfying:

$$\alpha^{2}(\nabla \overline{\mathbf{u}}_{h}^{n}, \nabla \mathbf{v}) + (\overline{\mathbf{u}}_{h}^{n}, \mathbf{v}) = (\mathbf{u}_{h}^{n}, \mathbf{v}),$$

$$\frac{1}{\Delta t}(\mathbf{u}_{h}^{n+1} - \mathbf{u}_{h}^{n}, \mathbf{v}) + \nu a(\mathbf{u}_{h}^{n+1/2}, \mathbf{v}) + b^{*}(\mathbf{u}_{h}^{n+1/2}, \mathbf{u}_{h}^{n+1/2}, \mathbf{v}),$$

$$+ \chi(\mathbf{u}_{h}^{n+1/2} - \overline{\mathbf{u}}_{h}^{n+1/2}, \mathbf{v}) = (\mathbf{f}^{n+1/2}, \mathbf{v}),$$
(3.6)

and for the sensitivity solution, find \mathbf{s}_h^{n+1} and \mathbf{w}_h^n satisfying:

$$\alpha^{2}(\nabla \mathbf{w}_{h}^{n}, \nabla \mathbf{v}) + (\mathbf{w}_{h}^{n}, \mathbf{v}) = (\mathbf{s}_{h}^{n}, \mathbf{v}),$$

$$\frac{1}{\Delta t}(\mathbf{s}_{h}^{n+1} - \mathbf{s}_{h}^{n}, \mathbf{v}) + \nu a(\mathbf{s}_{h}^{n+1/2}, \mathbf{v}) + b^{*}(\mathbf{s}_{h}^{n+1/2}, \mathbf{u}_{h}^{n+1/2}, \mathbf{v}) + b^{*}(\mathbf{u}_{h}^{n+1/2}, \mathbf{s}_{h}^{n+1/2}, \mathbf{v}),$$

$$+(\mathbf{u}_{h}^{n+1/2} - \overline{\mathbf{u}}_{h}^{n+1/2}, \mathbf{v}) + \chi(\mathbf{s}_{h}^{n+1/2} - \mathbf{w}_{h}^{n+1/2}, \mathbf{v}) = 0.$$
(3.7)

The numerical analysis of (3.6) and (3.7) can be studied in [11, 27].

4 The Interval of Reliability

In this numerical study, we aim to show that the flow sensitivity calculated from sensitivity equations (3.3), (3.5), or (3.7) can be used to quantify the reliability of the flow solution computed using (3.2), (3.4), or (3.6) respectively as the user-elected model parameter takes different values. Let η be the designated model parameter, then one can look at the following difference quotient for the sensitivity,

$$\mathbf{s} = \frac{\partial \mathbf{u}}{\partial \eta} \approx \frac{\mathbf{u}(\eta) - \mathbf{u}(0)}{\eta} \tag{4.1}$$

Considering \mathbf{u} as an implicit function of parameter η , $\mathbf{u}(0)$ indicates the true solution of Navier-Stokes equations while $\mathbf{u}(\eta)$ for $\eta>0$ denotes the corresponding flow model approximation. In all the discussed fluid models in this paper, EVM, LAM, and TRM, the flow solution is an accurate approximation to the Navier-Stokes solution when $\|\mathbf{u}(\eta) - \mathbf{u}(0)\|$ is small, and according to (4.1) the accuracy of the model approximation can be estimated by measuring $\eta \|\mathbf{s}\|$. As noted in Section 3, the sensitivity calculation can be coupled with that of the original fluid model simulation. The computations for sensitivity equations are easily added as all of the data structures and filter calculations are very similar to that of the corresponding fluid model. Thus after computing a model simulation with a given set of parameters, the sensitivity computation can be done with only a nominal extra cost and a quantitative measure of reliability can be then calculated.

Note that in cases where the model parameter η corresponds to the filter width e.g. EVM and LAM, then $0 < \eta \le 1$, by selecting larger values of η , a larger set of velocity scales is removed. Hence, an approximated flow solution corresponding to large values of η may not be considered to be a reliable approximation to a solution of the Navier-Stokes model because too much of the small scale structure could be lost. This situation is especially tenuous for the case of high Reynolds numbers where the velocity contains a large number of small scales. Therefore, it is crucial to find the optimal balance between choosing a value of η that is small enough to provide a reliable approximation to the Navier-Stokes flow while choosing a value of η that is large enough so that the computation of the large scale velocity \mathbf{u} is feasible. This leads us to identify a range of η values for the interval of reliability for which both η and $\eta||\mathbf{s}||$ are small. With η as the parameter corresponding to filter width to determine the upper end of the interval of reliability, one can use the Taylor expansion taking η values so that $O(\eta^2)$ is of a certain precision,

$$\mathbf{u}(0) = \mathbf{u}(\eta) - \eta \mathbf{s} + O(\eta^2). \tag{4.2}$$

Next we present two numerical experiments with 2D Cavity problem where we specify reliable parameter values for LAM and TRM using the sensitivity computations as discussed in this section.

4.1 2D Cavity Problem

In the following experiments, two fluid models, LAM and TRM, and their sensitivity equations are numerically solved on the domain defined by $\Omega = [0,1] \times [0,1]$. The upper boundary condition is chosen to be $\mathbf{u} = (16x^2(1-x)^2,0)^T$ and zero everywhere else. The initial data is

 $\mathbf{u}(0,x,y) = (3y^2 - 2y,0)^T$ in Ω . Since initial and boundary conditions are independent from the model parameter η , they are set to zero for the sensitivity \mathbf{s} .

All the computations are carried out with a fixed mesh size $h = \frac{1}{36}$, and a uniform time step $\Delta t = 0.01$ using the Taylor-Hood finite elements. All the programs have been implemented using the software package FreeFem++; see [17] for details and examples.

Note that in the following computations, the sensitivity of the approximated velocity \mathbf{u} with respect to the variations of the model parameter is tested by computing $\|\mathbf{s}\|_{l^2(0,T;L^2)}$ (where

$$\|\mathbf{v}\|_{l^2(0,T;L^2)} = \left[\triangle t \sum_{i=0}^N \|\mathbf{v}(i\triangle t)\|_{L^p}^q \right]^{1/q}$$
 for final time $T = 1$.

4.1.1 Leray-Alpha Model

The sensitivity computations in this section are performed for different viscosities corresponding to Reynolds numbers of 5000, 10000, and 50000. In addition for each tested Re value, computations are carried out for variations of filter width α , where the values are chosen based on the spatial mesh size as $\alpha = kh$, for $k = \frac{1}{4}, \frac{1}{2}, 1, 2, 4$.

The numerical results obtained from these computations is shown in Figure 1. Note that by selecting large values for the parameter α , e.g. larger than 4h, all the velocity scales that are less or equal to α are filtered. Using (4.2), the reliable α values are restricted to values with $O(\alpha^2)$ less than 0.01. Considering the fact that a higher sensitivity for smaller values of parameter α indicates the rise of computational complexity, the numerical results in Figure 1 suggest the following interval of α values as the optimal choice for the tested Reynolds numbers.

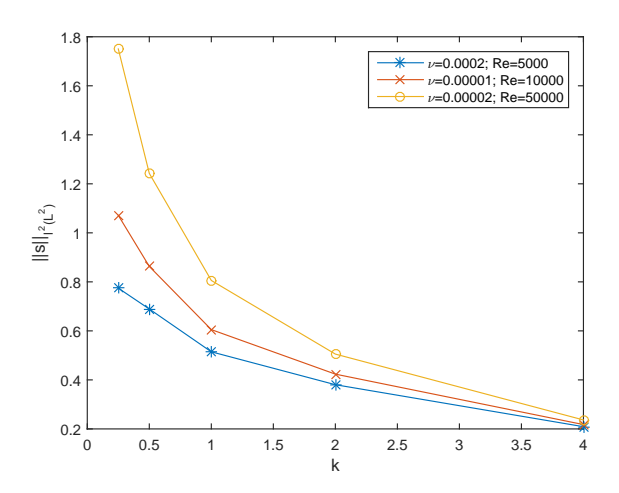


Figure 1: Sensitivity over the time interval of [0, 1]

As indicated in Table 1, the interval of optimal values of α for the best accuracy and computational complexity is smaller for higher Reynolds number.

Furthermore we present the sensitivity computations using the Forward Finite Difference (FFD) quotient $\frac{\mathbf{u}(\alpha+\Delta\alpha)-\mathbf{u}(\alpha)}{\Delta\alpha}$, by computing \mathbf{u} from (3.4) for two inputs $\alpha+\Delta\alpha$ and α . The goal is to illustrate a comparison of the sensitivity values obtained from FFD vesus that from sensitivity equation in (3.5) denoted by SEM for simplicity. The computations for sensitivity norm via both methods, $\|\mathbf{s}_{SEM}(t)\|_{L^2(\Omega)}$ and $\|\mathbf{s}_{FFD}(t)\|_{L^2(\Omega)}$, are performed for different α

Table 1: The interval of optimal values for parameter α

Re	Interval of α values
5000	$\frac{1}{4}h \le \alpha \le 4h$
10000	$\frac{1}{2}h \le \alpha \le 4h$
50000	$h \le \alpha \le 4h$

values with $\Delta \alpha = 0.001$ at times t = 0.1, and 1. Figures 2-4 display these computational results.

Note that for all α , sensitivities computed via FFD is overall larger than the one computed via SEM in all the tested Reynolds numbers. Sensitivity norm in both methods increases as α takes on values closer to 0 demonstrating a higher sensitivity of the approximated velocity \mathbf{u} with respect to smaller values of α . One also observes that as time has progressed from t=0.1 to t=1, sensitivities become larger in scale. In addition, larger Reynolds numbers show larger sensitivities especially at the final time.

The difference between $\|\mathbf{s}_{SEM}\|_{L^2(\Omega)}$ and $\|\mathbf{s}_{FFD}\|_{L^2(\Omega)}$ for different values of Reynolds number at t=1 is presented in Table 2. Sensitivity values for $\alpha=2h$, and 4h are apart up to 0.25 in all cases and there is an increase in the difference as α decreases. For high Reynolds number, i.e. Re=10000, and 50000, the difference in sensitivity norms is noticeable for $\alpha=\frac{1}{2}h$, and $\frac{1}{4}h$.

Table 2: Difference between $\|\mathbf{s}_{SEM}\|$ and $\|\mathbf{s}_{FFD}\|$ at t=1 with $h=\frac{1}{36}$

α	Re = 5000	Re = 10000	Re = 50000
4h	0.1586	0.1603	0.1586
2h	0.2458	0.2335	0.1955
h	0.4118	0.4315	0.3685
$\frac{1}{2}h$	0.4732	0.6689	0.9310
$\frac{1}{4}h$	0.4394	0.7133	1.4550

4.1.2 Time Relaxation Model

In this experiment, tested Reynolds numbers are 1000, 5000, and 10000, for different values of time relaxation parameter $\chi = 0.01, 0.1, 1,$ and 10.

As seen in Table 3, $\chi||\mathbf{s}||_{l^2(0,1;L^2(\Omega))}$ values via both methods take larger values for larger Re with any selected value of parameter χ . For Re = 1000, we suggest $\chi \leq 1$ as the best choice of accuracy while for larger Re values, we select a smaller interval of χ values, that is $\chi \leq 0.1$.

Remark 4.1. In this experiment, we chose χ values for which $\chi||\mathbf{s}||_{l^2(0,1;L^2(\Omega))} \leq 0.01$ for the best accuracy. The smaller χ values becomes, the more accurate calculations of approximated velocity \mathbf{u} becomes. However very small values of parameter χ results in increasing the

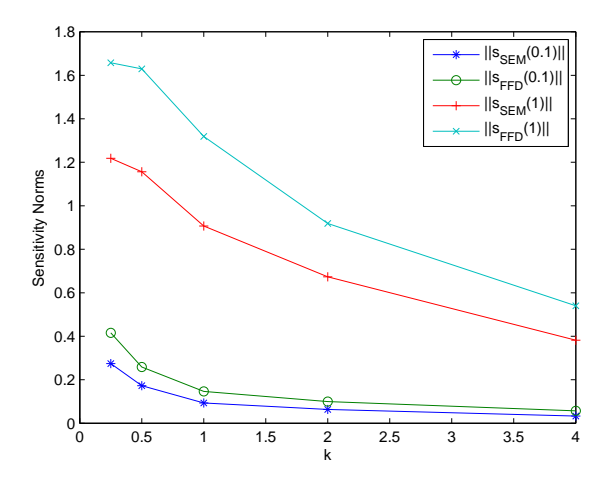


Figure 2: Sensitivity norms via SEM and FFD for Re=5000

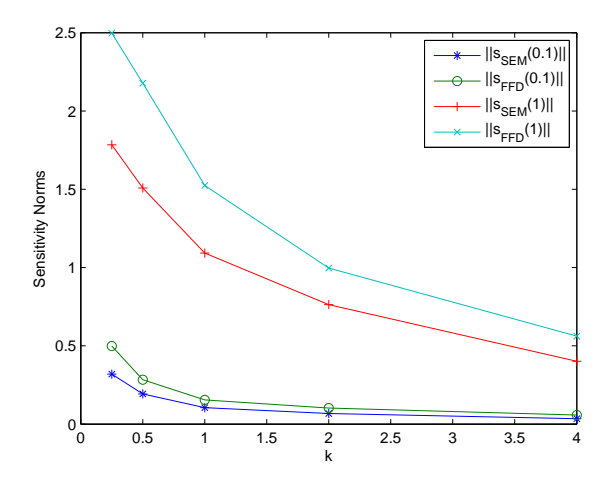


Figure 3: Sensitivity norms via SEM and FFD for Re=10000

Table 3: Sensitivity values $\chi \|\mathbf{s}\|_{l^2(0,1;L^2)}$

χ	Re = 1000	Re = 5000	Re = 10000
0.01	0.000106756	0.000191289	0.0002248
0.1	0.00103614	0.00184001	0.00215508
1	0.00803338	0.0131381	0.0149263
10	0.0503827	0.060064	0.0621485

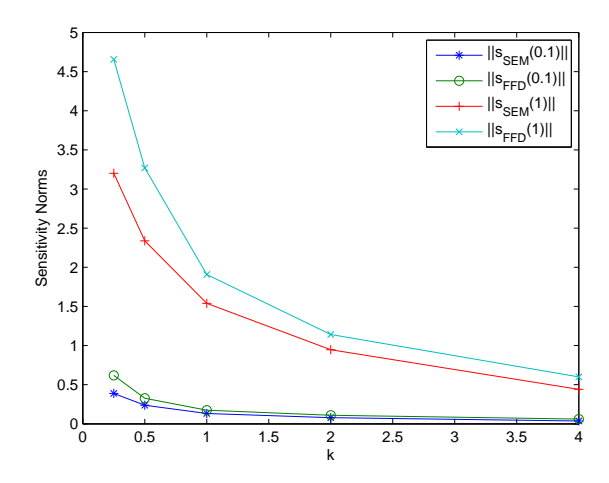


Figure 4: Sensitivity norms via SEM and FFD for Re = 50000

complexity of flow structures/scales that cannot be supported by the grid/mesh and thus numerical pollution of the computed velocity starts. Therefore, the user must consider the trade-off between increased accuracy and computational flow complexity when choosing the χ value.

The data listed in Tables 4-5 displays the maximum sensitivity values, i.e. $||\mathbf{s}||_{L^{\infty}(0,1;L^{2}(\Omega))}$, over the time interval [0, 1] for Re = 1000, and 10000 with different χ values as the spatial mesh size is refined. It is worth mentioning that the maximum sensitivity norm happens at the final time for any mesh size as well as any selected χ values. One observes a decrease in $||\mathbf{s}||_{L^{\infty}(0,1;L^{2}(\Omega))}$ as the spatial mesh size is refined for $\chi \leq 1$. In both tables, $||\mathbf{s}||_{L^{\infty}(0,1;L^{2}(\Omega))}$ values for $\chi = 10$ stay close through the mesh refinement.

Table 4: Sensitivity computations for Re = 1000 with mesh refinement

χ	$h = \frac{1}{9}$	$h = \frac{1}{18}$	$h = \frac{1}{36}$
0.01	0.0586237	0.035002	0.0157713
0.1	0.0541932	0.0330563	0.0151647
1	0.0250335	0.0199503	0.0110461
10	0.00893807	0.00966404	0.00747537

4.2 Improving Flow Functionals

The standard procedure of computing a flow functional is to first compute the approximated flow velocity \mathbf{u} from the fluid model, then use \mathbf{u} as the fluid velocity input into the given flow functional. Let η be the model parameter upon which \mathbf{u} depends implicitly with property that $\mathbf{u}(\eta) \to \mathbf{u}(0)$ as $\eta \to 0$. Let $J(\mathbf{u}(0)) = J(\mathbf{u})$ be a flow functional and that $\mathbf{u}(0)$ is extremely computationally expensive to obtain directly. The natural approach to compute a less expensive approximation of $J(\mathbf{u})$ is to calculate $J(\mathbf{u}(\eta))$ for a non-zero η . Note that $J(\mathbf{u}(\eta))$

Table 5: Sensitivity computations for Re = 10000 with mesh refinement

χ	$h = \frac{1}{9}$	$h = \frac{1}{18}$	$h = \frac{1}{36}$
0.01	0.0808053	0.0595574	0.0363773
0.1	0.0747136	0.0557121	0.0344382
1	0.0347436	0.0307948	0.02162
10	0.0094678	0.0106285	0.0090533

is a good approximation provided that $\mathbf{u}(\eta)$ is a good approximation and that the unresolved scales do not influence the functional. In this section, we discuss how the approximation of $J(\mathbf{u})$ can be improved by integrating sensitivities into the computations of the flow functional. The idea is simply based on the first order Taylor expansion of the flow functional around a non-zero η value. Expanding $J(\mathbf{u})$ around a non-zero η implies that

$$J(\mathbf{u}) \approx J(\mathbf{u}(\eta)) - \eta J'(\mathbf{u}(\eta)) \cdot \mathbf{s}$$
 (4.3)

Replacing J' by J, given J' = J for linear functionals, and incorporating the pressure into the above formula, the approximation (4.3) is rewritten as

$$J(\mathbf{u}, p) \approx J(\mathbf{u}(\eta), p(\eta)) - \eta J(\mathbf{s}, r) = J(\mathbf{u}(\eta) - \eta \mathbf{s}, p(\eta) - \eta r)$$
(4.4)

By (4.4), a flow functional can be approximated using sensitivities as the first order correction term for both the velocity and pressure.

This idea was proposed by Anitescu and Layton for LES models and was tested on the Smagorinsky model in [3].

Next we provide a numerical support for the idea that uses drag computations in a channel with a cylinder.

4.3 2D Flow around Cylinder

In this numerical experiment, we consider estimating drag functional using EVM on the standard test problem of two-dimensional flow in a channel around a cylinder.

The lift and drag functional for Navier-Stokes equations is given by

$$J(\mathbf{u}, p) = \int_{D} \hat{n} \cdot (pI - 2\nu \nabla^{s} \mathbf{u}) \cdot \hat{a} ds$$
 (4.5)

where \hat{n} denotes the normal vector on the cylinder boundary D directing into the channel, $\nabla^s \mathbf{u}$ presents the deformation tensor and is $\frac{1}{2}(\nabla \mathbf{u} + \nabla \mathbf{u}^T)$, the unit vector \hat{a} in the positive direction of x-axis or negative direction of y-axis yield the drag or lift flow functional.

Figure 5 displays the geometry of the channel with the cylinder. The channel is a rectangle with height and width as 0.41m and 2.2m respectively. The cylinder, denoted by D, is of radius 0.05m, and its center is placed at (0.2, 0.2).



Figure 5: Geometry of 2D-flow around cylinder

The numerical approximation to the solution of EVM in (2.1) are computed for $0 \le t \le 4$ with the inflow conditions given below that are parabolic in space and periodic in time

$$\mathbf{u}_{1}(t,0,y) = \frac{6}{(0.41)^{2}}y(0.41-y)\sin(\pi t)$$

$$\mathbf{u}_{2}(t,0,y) = 0.$$
(4.6)

A free condition is used for the outflow boundary condition, and the remaining boundary and initial conditions are given by

$$\mathbf{u}_{1}(t, x, 0) = \mathbf{u}_{2}(t, x, 0) = 0$$

$$\mathbf{u}_{1}(t, x, 0.41) = \mathbf{u}_{2}(t, x, 0.41) = 0$$

$$\mathbf{u}_{1}(t, x, y) \mid_{\partial D} = \mathbf{u}_{2}(t, x, y) \mid_{\partial D} = 0$$

$$\mathbf{u}_{1}(0, x, y) = \mathbf{u}_{2}(0, x, y) = 0.$$

A non-uniform mesh that is finer around the cylinder D is used for the triangulation of the domain in Figure 5. A given mesh is constructed using two sizes, h_1 for the sides of the channel, and h_2 for the boundary of D. Therefore the mesh is identified using the ordered pair (h_1, h_2) . For the numerical computation of the projection operator in (3.2) and (3.3), the applied coarse mesh has the same structure and is always chosen as $(H_1 = \sqrt{h_1}, H_2 = \sqrt{h_2})$. An example of a mesh of size $(\frac{1}{36}, \frac{1}{49})$ is indicated in Figure 3.

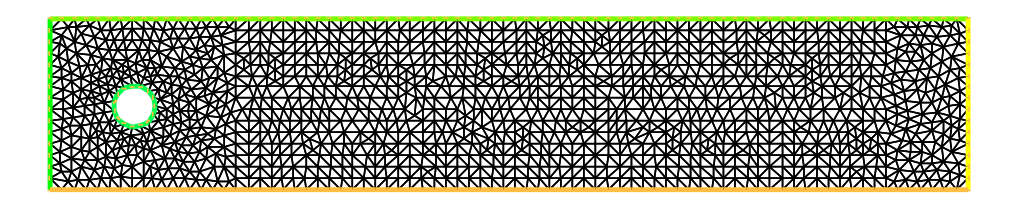


Figure 6: Mesh in a channel of size $(\frac{1}{36}, \frac{1}{49})$

The reference value of drag for this test problem is calculated using the DNS method on a fine mesh of size $(\frac{1}{100}, \frac{1}{121})$ for $0 \le t \le 4$. Figure 7 presents a sample of the scaled velocity vector field for the case when Re = 1000 and $\alpha = 0$ at t = 0.5. Note that this graph contains only the portion of the domain surrounding the cylinder where the interesting flow behavior occurs.

Table 6 lists the reference values of maximum drag, and the error in its estimation using the approximated large eddy velocity and pressure $(\mathbf{u}(\alpha), p(\alpha))$ and $(\mathbf{u}(\alpha) - \alpha \mathbf{s}, p(\alpha) - \alpha r)$ in

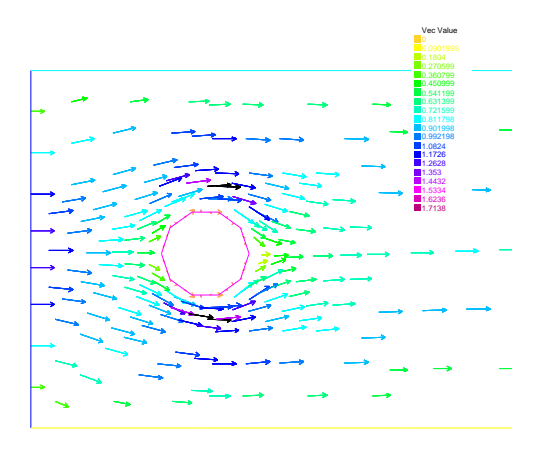


Figure 7: Velocity vector field for Re = 1000 and $\alpha = 0$

drag calculation by (4.5) for different values of Re. In this experiment, the approximated flow variables and their sensitivities are obtained from (3.2) and (3.3) with $\alpha = 0.00125$ and a mesh size of $(\frac{1}{49}, \frac{1}{64})$. As indicated in this table, computed drag values by $(\mathbf{u}(\alpha) - \alpha \mathbf{s}, p(\alpha) - \alpha r)$ are more accurate for all Re, especially for $Re \geq 100$. In addition the computed drag values using $(\mathbf{u}(\alpha) - \alpha \mathbf{s}, p(\alpha) - \alpha r)$ shows only a small improvement in comparison to the ones computed using $(\mathbf{u}(\alpha), p(\alpha))$ when $Re \leq 10$. However, for $Re \geq 100$, the errors incurred by using $(\mathbf{u}(\alpha) - \alpha \mathbf{s}, p(\alpha) - \alpha r)$ improve decrease by a full order of magnitude.

Table 6: Maximum drag values and the errors

	Max. Drag	Error using $(\mathbf{u}(\alpha), p(\alpha))$	Error using $(\mathbf{u}(\alpha) - \alpha \mathbf{s}, p(\alpha) - \alpha r)$
Re	$J(\mathbf{u},p)$	$ J(\mathbf{u},p) - J(\mathbf{u}(\alpha),p(\alpha)) $	$ J(\mathbf{u},p) - J(\mathbf{u}(\alpha) - \alpha \mathbf{s}, p(\alpha) - \alpha r) $
1	63.7703	0.4037	0.3702
10	41.1958	0.3628	0.3555
100	36.0677	0.389	0.0152
1000	35.29035	0.28095	0.02095
10000	35.1186	0.4354	0.0154

We examined the norm of the sensitivity quantities for the same range of Re values in Table 6. The sensitivity norms in Table 7 are negligible for $Re \leq 10$ indicating that the approximated flow solution is accurate for that range of Re values. As also reflected in Table 6, there is a nominal error in the drag value approximations using $(\mathbf{u}(\alpha), p(\alpha))$ for $Re \leq 10$. According to Table 7, for large values of Re, i.e. $Re \geq 100$, the flow becomes more sensitive, and using sensitivity information improves the estimated values of the drag functional significantly.

Table 7: Sensitivity for different values of ν

Re	$\ \alpha\ _{L^{\infty}(0,T;L^2)}$
1	7.19057e-06
10	2.88244e-04
100	0.00483735
1000	0.0155576
10000	0.0201101

5 Concluding Remarks

In this paper, we introduced CSEM for three fluid models, EVM, LAM and TRM. Obtaining the sensitivity equations, we developed numerical schemes for simulating the fluid models and their corresponding sensitivity. Once the numerical algorithm for solving each fluid model is implemented, the sensitivity calculations can be easily added due to the similarity in data structure. Our numerical experiments illustrate the application of sensitivities in quantifying model error arising from the choice of various parameter values and identifying those values that produce a reliable approximated velocity. The numerical results show that a smaller interval of reliable parameter values is obtained for larger values of Re. In addition, the sensitivity information is shown to be useful in increasing the accuracy of flow functionals for a nominal amount of effort in calculating sensitivities. Future studies can include stochastic finite element discretization that should give more insights into the parameter sensitivity.

References

- [1] N. A. Adams and S. Stolz, Deconvolution methods for subgrid-scale approximation in large eddy simulation, *Modern Simulation Strategies for Turbulent Flow*, 2001.
- [2] N. A. Adams and S. Stolz, A subgrid-scale deconvolution approach for shock capturing, *Journal of Computational Physics*, 178: 391-426, 2001.
- [3] M. Anitescu and W. Layton, Sensitivities in Large Eddy Simulation and Improved Estimates of Turbulent Flow Functionals, SIAM Journal of Scientific Computing, 29: 1650-1667, 2007.
- [4] J. Borggaard and J. Burns, A Sensitivity Equation Approach to Shape Optimization in Fluid Flows, *Flow Control*, 49-78, 1995.
- [5] J. Borggaard, D. Pelletier and E. Turgeon, Sensitivity and uncertainty analysis for variable property flows, in *Proceedings of the 39th AIAA Aerospace Sciences Meeting and Exhibit*, 0140, 1993.
- [6] J. Borggaard, D. Pelletier and E. Turgeon, A Continuous Sensitivity Equation Method for Flows with Temperature Dependent Properties, AIAA/USAF/NASA/ISSMO Symposium on Multidisciplinary Analysis and Design, 4821, 2000.

- [7] A. Bowers and L. Rebholz, Increasing accuracy and efficiency in FE computations of the Leray-deconvolution model, *Numerical Methods for Partial Differential Equations*, to appear.
- [8] V.V.Chepyzhov, E.S. Titi and M.I. Vishik, On the convergence of the Leray-alpha model to the trajectory attractor of the 3d Navier-Stokes system, Report, 2005.
- [9] A. Cheskidov, D.D. Holm, E. Olson and E.S. Titi, On a Leray-α model of turbulence, Royal Society London, Proceedings, Series A, Mathematical, Physical and Engineering Sciences, 461, 2005, 629-649.
- [10] L. Davis and F. Pahlevani, Semi-Implicit Schemes for Transient for Navier-Stokes Equations and Eddy Viscosity Models, Journal of Numerical Methods for Partial Differential Equations, 25 (2009), 212-231.
- [11] S. De, D. Hannasch, M. Neda and E. Nikonova, Numerical analysis and computations of a high accuracy Time Relaxation fluid flow model, *International Journal of Computer Mathematics*, 1-22, 2008.
- [12] A. Dunca and Y. Epshteyn, On the Stolz-Adams deconvolution LES model, SIAM Journal on Mathematical Analysis, 2006.
- [13] V. J. Ervin, W. J. Layton and Monika Neda, Numerical Analysis of a Higher Order Time Relaxation Model of Fluids, *International Journal of Numerical Analysis and Modeling*, 4, 648-670, 2007.
- [14] A.Godfrey, E. Cliff and W. Eppard, Using Sensitivity Equations For Chemically Reacting Flows, AIAA/USAF/NASA/ISSMO Symposium on Multidisciplinary Analysis and Optimization, 4805, 1998.
- [15] V. Girault and P. Raviart, Finite element approximation of the Navier-Stokes equations, Springer, (1979).
- [16] M. Gunzburger, Perspectives in Flow Control and Optimization, Frontiers in Mathematics, SIAM, Philadelphia, 2003.
- [17] F. Hecht, O. Pironneau and K. Oshtsuka, Software Freefem++, http://www.freefem++.org, 2003.
- [18] A.A. Ilyin, E.M. Lunasin and E.S. Titi, A modified Leray-alpha subgrid-scale model of turbulence, Report, 2005.
- [19] V. John, Large Eddy Simulation of Turbulent Incompressible Flows, Springer 2004.
- [20] S. Kaya and B. Riviere, Analysis of a discontinuous Galerkin and eddy viscosity method for Navier-Stokes Equations, SIAM Journal of Numerical Analysis, 43 (2005), 1572-1595.
- [21] W. Layton, A connection between subgrid scale eddy viscosity and mixed methods, Applied Mathematics and Computing, 133 (2002), 147-157.

- [22] W. Layton and L. Rebholz, Approximate Deconvolution Models of Turbulence: Analysis, Phenomenology and Numerical Analysis, Springer Lecture Notes in Mathematics, 2012.
- [23] W. Layton, C. Manica, M. Neda and L. Rebholz, Numerical Analysis and Computational Testing of a high-order Leray-deconvolution turbulence model, *Numerical Methods for Partial Differential Equations*, 24(2008), 555-582.
- [24] J. Leray, Essay sur les mouvements plans d'une liquide visqueux que limitent des parois, J. math. pur. appl., Paris Ser. IX, 13(1934), 331-418.
- [25] J. Leray, Sur les mouvements d'une liquide visqueux emplissant l'espace, *Acta Math.*, 63(1934), 193-248.
- [26] M. Neda, F. Pahlevani and J. Waters, Sensitvity computations of the Leray-α model, Contemporary Mathematics, Recent Advances in Scientific Computing and Applications, 586: , 2013.
- [27] M. Neda, F. Pahlevani and J. Waters, Sensitvity analysis and computations of Time Relaxation Model, Advances in AppliedMathematics and Mechanics, 7 (1): 89-115, 2015.
- [28] F. Pahlevani and L. Davis, Parameter Sensitivity of an Eddy Viscosity Model: Analysis, Computation and its Application to Quantifying Model Reliability, *International Journal of Uncertainty Quantification*, 3 (5): 397-419, 2013.
- [29] F. Pahlevani, Sensitivity Computations of Eddy Viscosity Models with an Application in Drag Computation, *International Journal for Numerical Methods in Fluids.*, 52-4:381-392, 2006.
- [30] Ph. Rosenau, Extending hydrodynamics via the regularization of the Chapman-Enskog expansion, *Phys. Rev.*, A 40(1989), 7193.
- [31] P. Sagaut, Large Eddy Simulations for Incompressible Flows, Springer 2006.
- [32] S. Schochet, and E. Tadmor, The regularized Chapman-Enskog expansion for scalar conservation laws, Arch. Rat. Mech. Anal., 119(1992), 95.
- [33] M.I. Vishik, E.S. Titi and V.V. Chepyzhov, Trajectory attractor approximations of the 3d Navier-Stokes system by the Leray-alpha model, *Russian Math Dokladi*, 71(2005), 91-95.